# High-density Stark profiles of two neutral helium lines and their forbidden components*

J. R. Greig† and L. A. Jones‡
*Department of Physics and Astronomy, University of Maryland, College Park, Maryland 20742*

R. W. Lee§
*Physics Department, Imperial College of Science and Technology, London, SW7, England*
(Received 5 February 1973; revised manuscript received 23 August 1973)

Measured and calculated profiles are compared for the two neutral helium lines, He I ($\lambda = 4471$ and $\lambda = 6678$ Å) and their forbidden components at electron densities between $1.6 \times 10^{17}$ and $4.4 \times 10^{17}$ $cm^{-3}$. The partially ionized helium plasma was created in the reflected shock of an electromagnetically driven $T$ tube. The electron temperature was measured as $\sim 25\,000$ °K. The calculated profiles include a random-phase approximation for the electrons to second-order in the frequency-dependent shift and width operators, and the quasistatic approximation for the ions. Calculations were done at the measured plasma conditions and are compared directly with the experimental profiles. Agreement between theory and experiment is good even though in this density range the line He I ($\lambda = 6678$ Å) passes from the "isolated-line" to the "overlapping-line" regime, while the line He I ($\lambda = 4471$ Å) passes from the "overlapping-line" to the "degenerate-hydrogenic" regime.

## I. INTRODUCTION

Now that it is generally accepted that the GBKO (Ref. 1) type[2,3] calculations adequately describe the shapes of isolated neutral helium lines, more attention has been focused on the overlapping neutral helium lines. Because of its astrophysical interest, the line He I ($\lambda = 4471$ Å, $4\,^3D$-$2\,^3P$), has received the most attention.[4-6] But in many laboratory plasmas this line is also interesting because the "forbidden component" ($\lambda = 4470$ Å, $4\,^3F$-$2\,^3P$) has become as intense as the allowed line. The broadening of the combined line should then be described by a hydrogenic calculation similar to that of $H_\beta$ and the line should become a useful diagnostic for these high-density plasmas.

The line HeI ($\lambda = 6678$ Å, $3\,^1D$-$2\,^1P$) has received far less attention, but in these same high-density laboratory plasmas this line becomes interesting because the $3\,^1P$ energy level begins to mix with the $3\,^1D$ level, thus requiring the line to be treated by an overlapping-line theory. This mixing of energy levels permits emission in the forbidden line $\lambda = 6632$ Å, $3\,^1P$-$2\,^1P$, and a consequent decrease in the broadening of the allowed line. Even when the peak intensity in the forbidden line (measured above the wing of the allowed line) is only $\sim \frac{1}{10}$ the peak intensity of the allowed line, the width of the allowed line is already decreased from the would-be isolated line width by ~15%.

The range of electron densities covered in this work is such that we observe both the change from isolated to overlapping for the line $\lambda = 6678$ Å and from overlapping to completely degenerate for the line $\lambda = 4471$ Å. Thus we provide a comparison between theory and experiment in the critical transition regions at both ends of the overlapping line regime. At the same time, we extend the comparison between theory and experiment to electron densities not covered in previous experiments.[7-12]

It should be pointed out that the formalism used here to calculate the profiles incorporates frequency-dependent shift and width operators and that the distinction between isolated, partially overlapping, and degenerate lines is academic.

## II. APPARATUS AND EXPERIMENTAL PROCEDURE

The $T$-type shock-tube apparatus used in this work was used previously by Elton and Griem.[13] For this work it had a Pyrex expansion tube approximately 85 cm long and 25-mm inside diameter. Helium gas was leaked in through the electrodes and was pumped out through two small holes diametrically opposite each other located approximately 3 mm in front of the reflector (Fig. 1). After each shot the tube was pumped out to about 10 mTorr using a rotary pump and liquid-nitrogen trap via the inlet port at the electrodes, and a burst of gas was flushed in at $B$ to prevent debris collecting in the two small holes (~0.5 mm diam).

Observations were made on the partially ionized helium plasma produced in the reflected shock through these two small holes along the optic axis $AA$. By operating in this way with the Pyrex

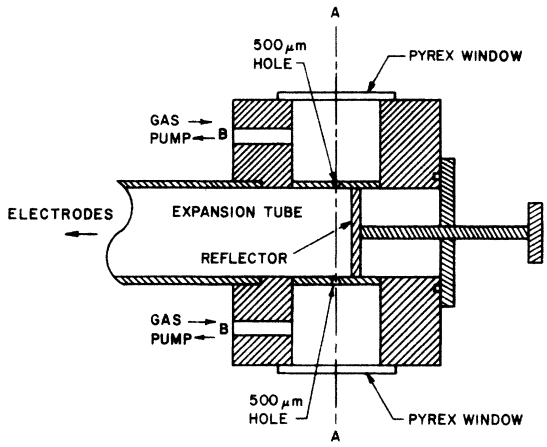


FIG. 1. Schematic representation of the reflector end of the $T$ tube. Measurements were made by viewing spectroscopically along axis $AA$.

windows separated from the plasma by about 5 cm of low-pressure (~1 mTorr) helium, we removed the problem of having either a cold boundary layer or rapidly deteriorating windows.

The shock tube was energized by the same 108-$\mu$F capacitor bank used by Elton and Griem. However, to maintain good reproducibility over large numbers of shots (~70) we ran a low-current glow discharge in the $T$-tube prior to firing by connecting a 10-M$\Omega$ resistor in parallel with the seven spark-gap switches. This only became necessary after we had replaced the air-filled spark gaps with pressurized gaps filled with dry nitrogen. In all these runs the capacitor bank was charged to +9 kV and the spark gaps were triggered by applying a pulse of −15 kV to the parallel connected trigger pins. The three different plasma conditions were obtained by varying the filling pressure of the shock tube as shown in Table I.

Four monochromators were used simultaneously in all runs, two on each side of the shock tube. Two of the monochromators, one on each side, were used as reproducibility monitors. One of these observed the total intensity in the neutral helium line HeI ($\lambda = 3889$ Å). This line has similar upper-state excitation energy to the two lines being studied and therefore has the same temperature dependence. The other monitor observed the continuum intensity at a wavelength of 5200 Å. By observing the gradual decay (30% per run) of both monitors we were able to correct for the dirtying of the windows. In practice, the continuum intensity and the two line intensities were both corrected to constant $\lambda = 3889$ Å intensity,

$$I(\text{corr}) = \frac{I(\text{meas})}{I_{3889}(\text{meas})}\, I_{3889}(\text{av}).$$

Then shots for which the continuum intensity fell outside the range ±20% of the average continuum intensity were discarded. Less than ~5% of the shots were discarded for this reason. Of course some shots (~5%) were discarded because of abnormal variations in the $\lambda = 3889$ Å monitor and very occasionally for gross misfiring.

Such misfirings were readily detectable by the change of shape of the intensity-time variation of the monitors. In a normal shot the intensity rose in ~0.5 $\mu$sec, remained constant for ~2 $\mu$sec, then

TABLE I. Summary of diagnostics.

| Fill pressure (cm of oil) | Scan No. | Wavelength of line (Å) | $N_e$ (units of $10^{17}$ cm$^{-3}$) Continuum | Width | Temperature (units of $10^3$ °K) Line intensity | Line to cont. ratio | Averaged $N_e$ (cm$^{-3}$) | Averaged temperature (°K) |
|---|---|---|---|---|---|---|---|---|
| 33.5 | 1 | 6678 | 1.7 | 1.4 | 21.7 | 22.7 | $1.6\times10^{17}$ | $2.4\times10^4$ |
| | | 4471 | ...[a] | 1.2[b] | 17.3 | ...[a] | | |
| | 2 | 6678 | 1.8 | 1.4 | 26.6 | 29.0 | | |
| | | 4471 | ...[a] | 1.2[b] | 26.9 | ...[a] | | |
| 22.5 | 3 | 6678 | 5.5[c] | 3.3 | 27.1 | ...[c] | $3.4\times10^{17}$ | $2.4\times10^4$ |
| | | 4471 | ...[a] | 3.6 | 20.6 | ...[a] | | |
| | 4 | 6678 | 5.6[c] | 3.3 | 25.5 | ...[c] | | |
| | | 4471 | ...[a] | 3.4 | 21.1 | ...[a] | | |
| 14.0 | 5 | 6678 | 4.0 | 3.7[d] | 28.0 | 25.8 | $4.4\times10^{17}$ | $2.6\times10^4$ |
| | | 4471 | ...[a] | 3.9 | 22.0 | ...[a] | | |
| | 6 | 6678 | 5.0 | 3.7[d] | 28.0 | 28.5 | | |
| | | 4471 | ...[a] | 4.5 | 24.7 | ...[a] | | |

[a] Not displayed since continuum under the He I ($\lambda = 4471$ Å) line is uncertain due to the wings of other neutral helium lines.

[b] Not used in average since the upper level of the He I ($\lambda = 4471$ Å) line is not yet completely degenerate.

[c] Not used in average since continuum uncertain due to hydrogen impurity concentration.

[d] Not used in average since the upper level of the He I ($\lambda = 6678$ Å) line is no longer isolated.

rose to a nonreproducible level. We believe that the plateau region represented emission from the shock-heated helium plasma and this was followed by nonreproducible emission from the impurity-laden piston plasma. All line-profile measurements were made on the plateau. A very useful check on the reproducibility of the plasma conditions was the arrival time of the first luminous front (actually the reflected shock) preceding the plateau of intensity. The total time between the firing of the spark gap switches and the arrival of this luminous front at the observation point varied from 60 to 70 $\mu$sec with increasing filling pressure. Within any run the arrival time varied by less than $\pm 0.25$ $\mu$sec.

The other two monochromators were used to scan, on a shot-to-shot basis, the profiles of the two lines He I ($\lambda = 4471$ Å) and ($\lambda = 6678$ Å). The instrument widths ($\sim 0.5$ Å) were in both cases quite negligible. Absolute sensitivity calibrations were made using a tungsten ribbon lamp and an optical pyrometer.

Approximate electron temperatures were determined from the total line intensities for the two lines, He I ($\lambda = 4471$ Å) and ($\lambda = 6678$ Å) and the line to continuum ratio of $\lambda = 6678$ Å. These are given in Table I; their accuracy is not important because of the very weak dependence of the line shapes on temperature. For the line-shape calculations (Sec. III) a typical temperature of 25 000°K was accepted. Electron densities were determined from three separate calculations. First (i) we used the measured continuum intensity under the He I ($\lambda = 6678$ Å) line and our own calculations of the variation of this intensity with electron density using the equations given by Griem.[14] (These calculations agree within ±5% with those of Eberhagen and Lunow.[15]) Second (ii) we used the half-intensity width of the line He I ($\lambda = 4471$ Å) and the hydrogenic calculations by Griem.[16] And finally (iii) we used the half-intensity width of the line He I ($\lambda = 6678$ Å) and the GBKO calculations.[17] All three measurements for each of the three plasma conditions used in this work are given in Table I. At the lowest electron density ($N_e \sim 1.6 \times 10^{17}$ cm$^{-3}$) we used the averages of the electron densities measured by (i) and (iii). That obtained from (ii) we felt to be untrustworthy since the line He I ($\lambda = 4471$ Å) has not yet developed the full hydrogenic dependence on electron density. At the middle density ($N_e \sim 3.4 \times 10^{17}$ cm$^{-3}$), the electron density obtained from the half-widths of the two lines agree quite well, whereas that obtained from the continuum under He I ($\lambda = 6678$ Å) is too high. We believe the large observed continuum is due to the fact that these two scans were done first, immediately after the liquid-nitrogen cold trap was added to the pumping system. And therefore there was a considerable amount of hydrogen still impregnated in the tube walls. This would mean that the $H_\alpha$ wing is the cause of the anomalously high continuum measurement. This hypothesis is supported by the fact we observed a rise in intensity near $H_\alpha$ for these two scans. And at the high-density ($N_e \sim 4.4 \times 10^{17}$ cm$^{-3}$) measurements (i) and (ii) were averaged to obtain the electron density, since at this condition the broadening of He I ($\lambda = 6678$ Å) is no longer that of an isolated helium line and the electron density given by (iii) should now be too low. We have accepted the average electron densities given in column eight of Table I as the true plasma densities and calculated full line profiles for each of the two lines at these densities in order to compare theory and experiment.

The transition of the 6678-Å profile from one well described by an isolated line formalism to one requiring an overlapping line theory occurs at approximately a density of $3 \times 10^{17}$ cm$^{-3}$. This is estimated by comparing the splitting $\omega_{12}$ between the upper state of the line and its nearest perturbing level, with the quasistatic (half)-half-width $\omega_H$ whose upper state has the same principal quantum number $n$ as the line of interest.[18] Since $\omega_H$ will overestimate the width of a line whose upper state is not completely degenerate in $l$, the orbital quantum number, the electron density below which a line can be considered isolated is given by[19] (with $\omega_{12}$ in angular frequency units)

$$N_e = (\omega_{12}/1.2n^2)^{3/2} \text{ cm}^{-3}.$$

In the case of 4471, the levels $4\,^3D$, $4\,^3F$ become completely "degenerate" at about $3 \times 10^{17}$ cm$^{-3}$. Here the estimate used for the He I ($\lambda = 6678$ Å) line is inappropriate because we are interested in the change from partially overlapping to completely degenerate lines. Thus, since the hydrogen 2-4 transition $H_\beta$ is a completely degenerate line similar to He I ($\lambda = 4471$ Å), a good test of the transition to a degenerate regime is to compare when the He I ($\lambda = 4471$ Å) line becomes $H_\beta$-like. This is verified by comparing the $H_\beta$ profile with the profile of the He I ($\lambda = 4471$ Å) line for similar conditions and finding when the two profiles are in relative agreement from the wing to the region just inside the half-intensity points. To do this one can use either tabulated values or the asymptotic wing formula for $H_\beta$.

## III. THEORY

In order to calculate the line profiles of interest, approximations were employed in three areas. That is, approximations were used for (a) the atomic model, (b) the plasma model, and (c) their

mutual interaction. The majority of these assumptions have been used before, so their validity will not be discussed here, but, instead references will be given to the appropriate works.

In the case of the helium atom we specify its wave function as the representation of the model used. Here we assume that the independent-electron model is adequate and thus the total wave function for the two electron atom $\Psi_T(1, 2)$ is assumed to be of the form

$$\Psi_T(1, 2) = U(n_1 l_1 m_1) * U(n_2 l_2 m_2),$$

where the $U(nlm)$ is a hydrogenic wavefunction. It is also assumed that only one electron is optically active, so we have $\Psi_T = U(100) \times U(nlm)$. Further, when the hydrogenic radial matrix elements are significantly different from the Coulombic values, the Bates-Damgaard[20] correction factors are used to alter these values. For example, the radial matrix element for $\langle\langle 4p/R/4s\rangle\rangle^2$ is multiplied by a correction factor of ~0.85. A brief discussion of this model is given in Gieske and Griem.[6]

In the case of the lower level $2\,^3P$, there is a $j$ splitting of about one wave number[21] between the $J=0$ and $J=1, 2$ states. However, at the densities calculated in this paper this should not affect the outcome of the resultant calculations and therefore has been ignored.

The interaction between the plasma and the atom is most easily dealt with in terms of the static broadening and the dynamic (collisional) broadening separately. For the static-ion field, which is an infinite-order contribution in the interaction, the microfield distribution functions of Hooper[22] were used. In the only case, i.e., HeI ($\lambda = 4471$ Å) at $1.6 \times 10^{17}$ cm$^{-3}$, where it was felt the electrons might contribute statically we find that the static wing has not been reached. In all other cases we are closer to line center, thus implying that the neglect of static electrons will not affect the profiles significantly.

The Stark interactions involving the lower levels of the transitions are assumed to be negligible. This should be a good approximation due to the very large inherent spacing in the lower levels and the relatively large static broadening of the upper levels. The static broadening is calculated allowing for the upper levels $3\,^1S$, $^1P$ and $^1D$, and $4\,^3S$, $^3P$, $^3D$, and $^3F$.

For the plasma electrons we use a fully quantum-mechanical system. It is assumed that the interaction between the electrons and atoms is characterized, and dominated, by weak collisions, where "weak" is used in the sense of small momentum transfer. The validity of this assumption has been discussed,[1,2] and implies that the random-phase approximation (RPA) yields a good description of the electrons in the plasmas we are concerned with. For these calculations we have assumed that effects due to ion motion can be neglected.[23]

The dynamic, or collisional broadening, is treated perturbatively. Here the Dyson series, or equivalently the self-energy expansion, which describes the electrons in their perturbation of the atom, constitutes an infinite-order contribution in the exact atom-perturber interaction. Approximations are made to this self-energy expansion in two ways. First, the exact potential is expanded in terms of multipoles and then truncated. Second, the infinite-order perturbation series is expanded in terms of the approximate potential and also truncated.

The perturbation expansion is truncated after the first nonvanishing term, thus we have included second-order contributions to the line profile from the dynamic perturbation of the plasma electrons. In general this leaves us with "shift and width operators"[24] of the form

$$\int e^{i\Delta\omega t} \langle V_{ap}(t)\, V_{ap} \rangle_p dt, \tag{1}$$

where $\Delta\omega$ is separation from line center and $V_{ap}$ is the atom-plasma interaction. The $\langle\ \rangle_p$ represents the average over the plasma coordinates.

The multipole expansion for the exact atom-plasma interaction, $V_{ap}$, is then truncated after the dipole term. However, to verify the accuracy of this approximation the quadrupole term was calculated[3]; this will be discussed later. The potential of interest is then

$$V_{ap} = e^2 \frac{\vec{d}_A \cdot \vec{r}_p}{|\vec{r}_p|^3} + \frac{3(\vec{d}_A \cdot \vec{r}_p)^2 - \vec{r}_p^{\,2}\, \vec{d}_A^{\,2}}{2|\vec{r}_p|^5}, \tag{2}$$

where the first term is the perturber monopole-atomic dipole interaction and the second term is the monopole-quadrupole interaction.

Although the RPA treatment does not yield divergent shift and width operators, the strong collisions are incorrectly treated. Thus a minimum impact parameter is needed. The electron impact parameter was determined by requiring unitarity of the total shift and width operator, with the strong collision accounted for approximately. The Lorentz-Weiskopf term[1] is used to estimate the effects of strong collisions.

The collisional broadening is calculated for all the upper and lower levels concerned. Thus all the proper self-energy contributions are included, but the interference terms[25] which constitute the vertex corrections are ignored.

The theoretical accuracy of these approximations is discussed in detail by Griem.[4] To determine

the validity of the multipole truncation we evaluated the quadrupole effects on the shift and width operators. The evaluation of the appropriate matrix elements was carried out using the hydrogenic states. The contribution to the integral in Eq. (1) was treated approximately. Here the evaluation employed by Cooper and Oertel[3] was used. Further, considering the similarlity between the He I ($\lambda = 4471$ Å) profile and the $H_\beta$, hydrogen 2-4, transition, the estimate employed by Kepple and Griem,[26] for quadrupole effects, i.e., just the addition of a constant $\frac{4}{3} kT/E_H$ to the shift and width operator, serves as an independent verification of the truncation procedure. The results of these estimates show that the maximum contribution to the shift and width operator is *less* than 1% and this arises for the lowest density He I ($\lambda = 4471$ Å) profile. For here the dipole broadening is diminished by large separation from line center [Fig. 2(b)].

To estimate the accuracy of the truncation of the perturbation expansion, again the lowest density He I ($\lambda = 4471$ Å) is used as an example. For here exists the best possibility that the strong collisions will need detailed treatment. We estimate the percentage of the electrons that should be treated by higher-order terms in the dipole series pessimistically by evaluating[27]

$$N_e(\text{static}) = \int_0^{y_{\min}} f(y)\, dy, \tag{3}$$

where $y_{\min} \cong \hbar \rho_{\min}^2 \Delta\omega / 2KT$, and $f(y) = (2/\pi^{1/2}) y^{1/2} e^{-y}$. For the largest frequency separation of interest, this is found to be less than ~10% of the electrons for the lowest density He I ($\lambda = 4471$ Å) case. And it is lower for all other cases calculated.

The inclusion of lower-level broadening should reduce, but not appreciably, the estimate of 10% accuracy for the collisional broadening introduced by Griem.[4] In an analogous manner the accuracy of the static broadening should be limited to about 10%, the main inaccuracy arising from the approximate treatment of quadratic Stark effects and the neglect of levels with different principal quantum numbers.

## IV. RESULTS AND DISCUSSION

To compare the calculated line profiles with the experimental data, we have taken all the experimental data points below about 70% of the line peak intensity and fitted these points to the calculated profile. The fitting was done numerically[28] and on each line profile allowance was made for a constant continuum intensity under the line, a small error in the monochromator wavelength reading, and a constant factor relating the theoretical and experimental intensity scales. Unfortunately, absolute wavelength calibrations were only done at the beginning of the series of measurements and these were invalidated by severe increases in temperature on several occasions during the series. Therefore no absolute shift measurements have been made and the error in the monochromator wavelength reading varied by as much as 2 Å from run to run. Experimental points close to the line maximum intensity were not used in the fitting process because for the line He I ($\lambda = 4471$ Å) these points include the dip between the forbidden and allowed components, and for both lines there is always doubt about absorption or emission in the layer of gas between the windows and the plasma at the unshifted line center.

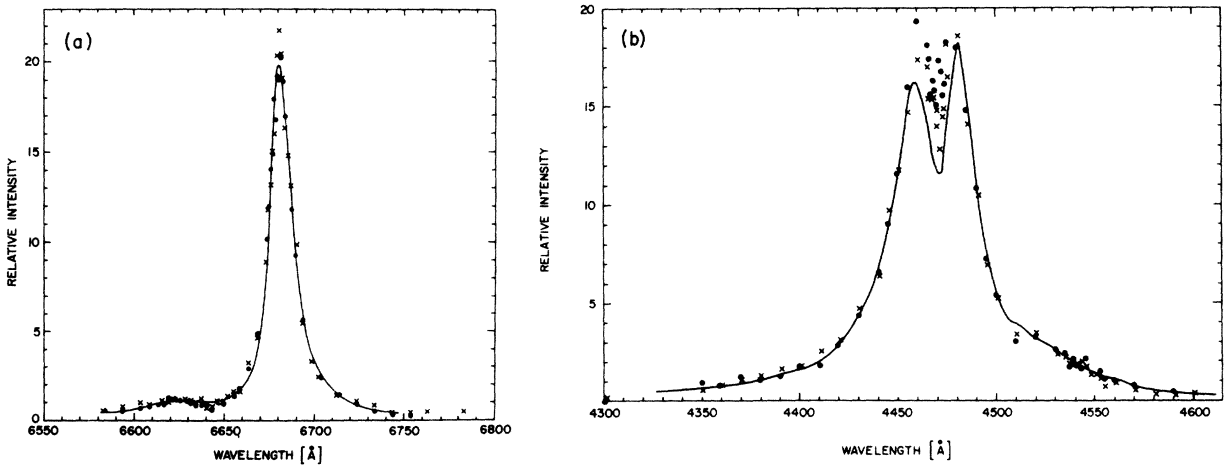


FIG. 2. Plot of relative intensity vs wavelength for two neutral helium lines: (a) He I ($\lambda = 6678$ Å) and (b) He I ($\lambda = 4471$ Å). Experimental points (×~ scan No. 1 and •~ scan No. 2) and calculated profiles (solid lines) are shown. The electron density equals ~ $1.6 \times 10^{17}$ cm$^{-3}$.

Figures 2–4 show the comparison between theory and experiment. In each case two quite separate sets of data points taken at the same shock-tube conditions (filling pressure, bank voltage, etc.) have been superimposed. The good agreement (± 20%) around the line maxima shows that there is in general very little boundary-layer problem. However, at the unshifted line center of HeI (λ = 6678 Å) there is often a sharp peak of emission or absorption due presumably to the low-density plasma in the gas between the plasma and the window. For HeI (λ = 4471 Å), although there is scatter in the data in the dip between the allowed and forbidden components, there is clearly no systematic difference between theory and experiment as is usually found with $H_\beta$.[29,30] However, there is a significant difference between theory and experiment for this line with regard to the intensity of the peak of the forbidden component at the lowest electron density ($1.6\times10^{17}$ cm$^{-3}$). Whereas in practice the two peaks are already equally intense, our calculation makes the forbidden component ~12% less intense. In this respect and in width, our calculated profile is in good agreement with those of Griem[4] and Barnard, Cooper and Shamey[5]. The excess measured intensity of the short wavelength maximum is comparable to the "blue" asymmetry of the $H_\beta$ line.[31]

The Stark interaction with the additional levels which affect these transitions, although not producing the over-all structure of the profile, does affect the profile's details. In the case of HeI (λ = 4471 Å) ($2\,^3P$-$4\,^3D$, $4\,^3F$) the forbidden line becomes more intense than the allowed line due to

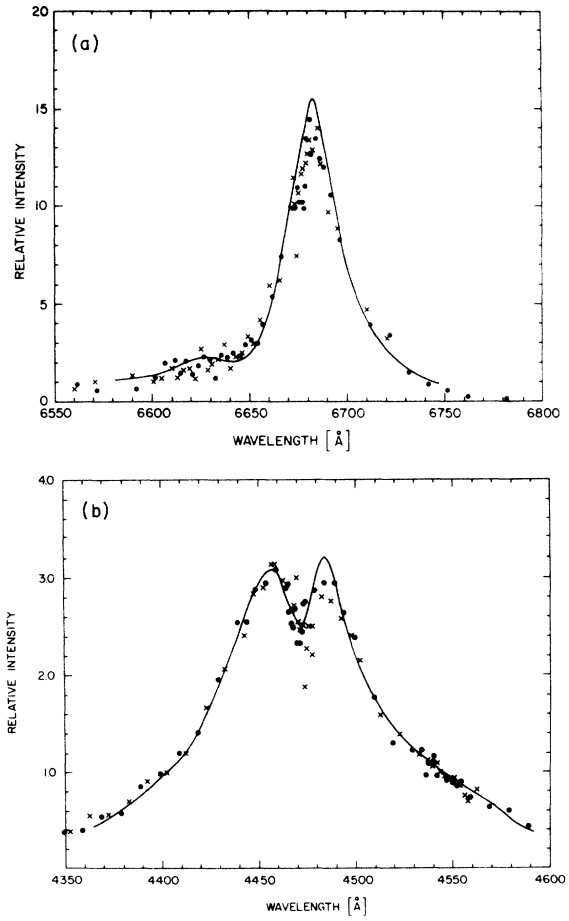


FIG. 3. Plot of relative intensity vs wavelength for two neutral helium lines: (a) HeI (λ = 6678 Å) and (b) HeI (λ = 4471 Å). Experimental points (× ~ scan No. 3 and ● ~ scan No. 4) and calculated profiles (solid lines) are shown. The electron density equals ~$3.4\times10^{17}$ cm$^{-3}$.

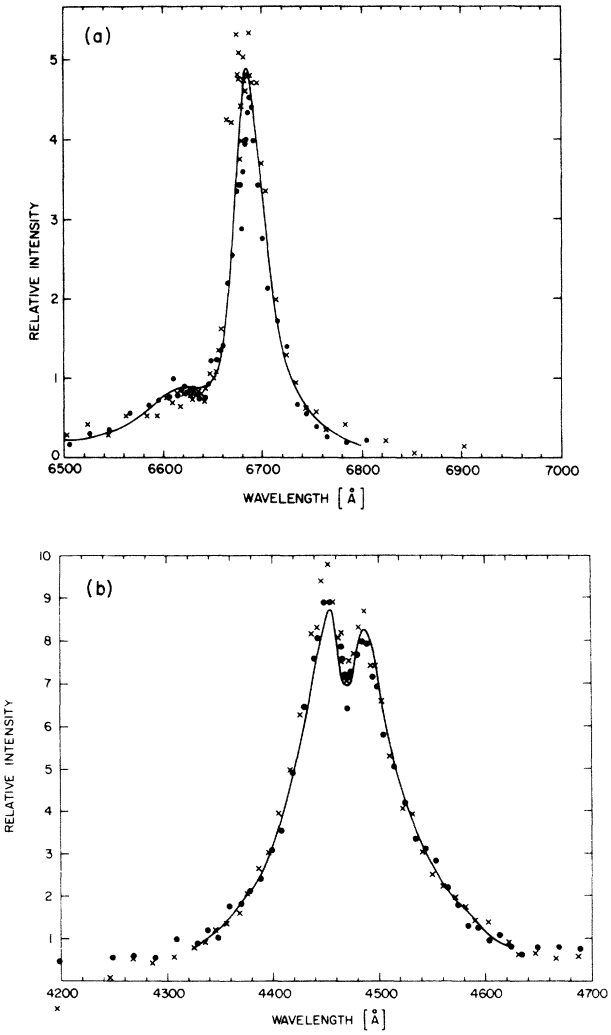


FIG. 4. Plot of relative intensity vs wavelength for two neutral helium lines: (a) HeI (λ = 6678 Å and (b) HeI (λ = 4471 Å). Experimental points (× ~ scan No. 5 and ● ~ scan No. 6) and calculated profiles (solid lines) are shown. The electron density equals ~$4.4\times10^{17}$ cm$^{-3}$.

the interaction $4\,^3P$-$4\,^3D$. The $4\,^3P$-$2\,^3P$ forbidden component is almost completely lost and does not come up in either theory or experiment. Again, this is largely due to the combined $4\,^3P$-$4\,^3D$, $4\,^3S$-$4\,^3P$ interactions. In the case of HeI ($\lambda = 6678$ Å) the forbidden component is increased in intensity due to the $3\,^1S$-$3\,^1P$ interaction. This is also the cause for the extended forbidden wing of this component.

It is clear from Figs. 2, 3 and 4 that within our experimental accuracy the theory used here adequately describes the broadening of both these lines even though the upper state of the one [HeI ($\lambda = 4471$ Å)] may be thought of as changing from an overlapping to a completely degenerate system, while the upper state of the other [HeI ($\lambda = 6678$ Å)] may be thought of as changing from an isolated to an overlapping system.

To compare these results with earlier work both on the lines of neutral helium[7-12] and on $H_\beta$,[28,29,30] we note that neglecting the effects of ion motion in the calculations has not caused significant discrepancies between measured and calculated profiles either in the forbidden component ($3\,^1P$-$2\,^1P$) of the singlet line (6678 Å) or in the dip of the triplet line (4471 Å). Although our measurements are made at higher electron densities than previous measurements and thus cannot be directly compared, the temperature of our plasma (~25000°K) is higher than those of Burgess and Cairns[8] and Birkeland *et al.*[9] and approximately equal to those of Jenkins and Burgess,[7] Ya'akobi *et al.*[11] and Bekefi *et al.*[12] Therefore, we would have expected to find similar discrepancies due to ion motion if the importance of this effect depended only on temperature (ion velocity). If on the other hand, the importance of ion motion were also density dependent[23] we should still have seen discrepancies similar to those found by Ya'akobi *et al.*[11] and Bekefi *et al.*[12] Since we do not see those discrepancies and yet our calculated profiles are in close agreement[23] with those of Griem[4] and Barnard, Cooper, and Shamey,[5] we suggest that previously reported discrepancies are not all due to ion motion. For instance, we believe the discrepancies between theory and experiment reported by Ya'akobi *et al.*[11] are in fact due to an error in the calculation of their theoretical profiles. Their experimental profiles are in good agreement with profiles one of us[32] has calculated for their plasma conditions and it has been found that their calculated profiles can be obtained by omitting the unshifted $2\,^1P(m = \pm 1)$-$3\,^1D(m - \pm 2)$ allowed component.

In comparing our measurements in the dip of the line HeI ($\lambda = 4471$ Å) with previous measurements on $H_\beta$, it is perhaps interesting that the neutral helium line is much less susceptible to boundary layer problems, because of its higher excitation potential, than $H_\beta$ and we find no systematic discrepancy with the neutral helium line in this experiment.

## ACKNOWLEDGMENTS

The authors wish to thank Dr. H. R. Griem for suggesting this problem and for many helpful discussions during the course of the work. Also they thank John Hey for his helpful assistance and discussions.

---

*This work is supported in part jointly by the National Aeronautics and Space Administration and the National Science Foundation.

†Present address: Imperial Chemical Industries, Slough, England.

‡Present address: Naval Research Laboratory, Washington, D. C.

§Present address: Mission Research Corp., Santa Barbara, Calif.

[1]H. R. Griem, M. Baranger, A. C. Kolb, and G. K. Oertel, Phys. Rev. 125, 177 (1962).

[2]H. R. Griem, *Plasma Spectroscopy* (McGraw-Hill, New York, 1964), Chap. 4. [For a more recent tabulation see S. M. Bennett and H. R. Griem, University of Maryland Technical Report No. 71-097 (unpublished).]

[3]J. Cooper and G. K. Oertel, Phys. Rev. 180, 286 (1969).

[4]H. R. Griem, Astrophys. J. 154, 1111 (1968).

[5]A. J. Barnard, J. Cooper and L. J. Shamey, Astron. Astrophys. 1, 28 (1969).

[6]H. A. Gieske and H. R. Griem, Astrophys. J. 157, 963 (1969). [See also H. A. Gieske, Ph.D. thesis (University of Maryland, 1968) (unpublished).]

[7]J. E. Jenkins and D. D. Burgess, J. Phys. B 4, 1353 (1971).

[8]D. D. Burgess and C. J. Cairns, J. Phys. B 4, 1364 (1971) [see also J. Phys. B 3, L67 (1970).]

[9]J. W. Birkeland, M. E. Bacon, and W. G. Braun, Phys. Rev. A 3, 354 (1971).

[10]R. H. Nelson and A. J. Barnard, J. Quant. Spectrosc. Radiat. Transfer 11, 161 (1971).

[11]B. Ya'akobi, E. V. George, G. Bekefi, and R. J. Hawryluk, J. Phys. B 5, 1017 (1972).

[12]G. Bekefi, E. V. George, and B. Ya'akobi, MIT Quarterly Progress Report (U.S.A.) No. 102, July, 1971 (unpublished), pp. 67–79.

[13]R. C. Elton and H. R. Griem, Phys. Rev. 135, A1550 (1964).

[14]H. R. Griem, Ref. 2, p. 113.

[15]A. Eberhagen and W. Lunow, Institut für Plasmaphysik Report No. IPP/1/23 June, 1964 (unpublished).

[16]H. R. Griem, Ref. 2, p. 303.
[17]H. R. Griem, Ref. 2, p. 88.
[18]H. R. Griem and K. Y. Shen, Phys. Rev. 122, 1440 (1961).
[19]J. Jenkins, Ph.D. dissertation (Imperial College, 1970) (unpublished).
[20]D. R. Bates and A. Damgaard, Phil. Trans. R. Soc. Lond. A 242, 101 (1949).
[21]W. C. Martin, J. Res. Natl. Bur. Stand. A64, 19 (1960).
[22]C. F. Hooper, Phys. Rev. 149, 77 (1966).
[23]R. W. Lee, J. Phys. B 6, 1044 (1973).
[24]U. Fano, Phys. Rev. 131, 259 (1968).
[25]M. Baranger, *Atomic and Molecular Processes*, edited by D. R. Bates (Academic, New York, 1962) Chap. 13.
[26]P. Kepple and H. R. Griem, Phys. Rev. 173, 317 (1968).
[27]H. R. Griem, Astrophys. J. 147, 1092 (1967).
[28]J. R. Greig and L. A. Jones, Phys. Rev. A 1, 1261 (1970).
[29]R. A. Hill and J. B. Gerardo, Phys. Rev. 162, 45 (1967).
[30]W. L. Wiese, D. E. Kelleher, and D. R. Paquette, Phys. Rev. A 6, 1132 (1972).
[31]H. R. Griem, Z. Phys. 137, 280 (1954).
[32]R. W. Lee, J. Phys. B (to be published).